RSC Advances

PAPER

View Article Online
View Journal | View Issue

Cite this: *RSC Adv.*, 2020, **10**, 27585

Formation of dialysis-free Kombucha-based bacterial nanocellulose embedded in a polypyrrole/PVA composite for bulk conductivity measurements†

Nadia Nirmal, Michael N. Pillay, Marco Mariola, Francesco Petruccione and Werner E. van Zyl*

The preparation of dialysis-free bacterial nanocrystalline cellulose (BNCC) combined with a suitable polymer to form a robust conducting material remains a challenge. In this work, we developed a polypyrrole@BNCC/PVA nanocomposite that avoids the time-consuming dialysis step and which exhibits bulk electrical conductivity. The nanocellulose (NC) was derived from bacterial cellulose (BC) that was grown from a symbiotic colony of bacteria and yeast (SCOBY) starting from Kombucha tea, and then subjected to sulfuric acid hydrolysis that led to isolable bacterial nanocrystalline cellulose (BNCC) product and subsequently utilized as a stabilizer and support. Pyrrole monomer was reacted with $FeCl_3 \cdot 6H_2O$ as a polymerization initiator to form polypyrrole (PPy) and combined with BNCC it produced PPy@BNCC nanocomposite. We found PPy to BNCC in a 1 : 1 ratio provided the best suspension of the components and formed a well dispersed homogeneous network. The PPy@BNCC nanocomposite was then suspended in polyvinyl alcohol (PVA), that facilitated the construction of a continuous PPy@BNCC/PVA conductive network in the matrix. We designed an in-house electrical measurement apparatus and developed a method that recorded bulk resistance. The results obtained from the measurements of the electrical properties of the PPy@BNCC/PVA composite prepared dialysis-free were then compared with (i) a dialyzed sample of similar composition, and (ii) a traditional four-point probe measurement. The PPy@BNCC/PVA dialysis-free sample showed a higher conductivity compared to the dialyzed composite at 4.27×10^{-1} and 3.41×10^{-1} S m^{-1}, respectively, and both values closely matched the traditional four-point probe measurement.

Received 26th May 2020
Accepted 17th July 2020

DOI: 10.1039/d0ra04649c

rsc.li/rsc-advances

Introduction

Cellulose is the most abundant biopolymer and renewable material on Earth and is formed by a variety of organisms such as plants, tunicates, fungi and bacteria.[1–3] Nanocellulose is a collective term for nanocrystals (nanocrystalline cellulose or cellulose nanofibrils) that remain after acid hydrolysis of wood or plant fiber.[4–7] Nanocellulose is typically in the shape of nanowhiskers or rods with a high aspect ratio (3–5 nm wide, 50–500 nm length) and is highly crystalline (60–90%).[8,9] Nanocellulose has emerged as a natural source for groundbreaking applications in materials science[10–12] and has demonstrated uses in diverse fields, including adsorbents for environmental remediation,[13] as hydrogels and aerogels,[14] as a suitable substrate for surface enhanced Raman scattering (SERS) studies,[15] for chemical and surface modifications on the cellulosic backbone,[16,17] as composite inks for 3D bioprinting,[18] as an iridescent chiral nematic material,[19] and several applications in biomedicine.[20–24]

During sulfuric acid hydrolysis of cellulose, the protic acid catalyzes the cleavage of a chemical bond by a nucleophilic substitution reaction[7] with sulfate groups ($R–OSO_3^-$) forming on the nanocellulose surface;[25] cleavage occur along the amorphous regions of the cellulose and upon sonication crystalline rod-like nanocellulose whiskers form. The nanocellulose is isolated from the waste hydrolysate *via* centrifugation and dialysis to remove the soluble sugars and residual acids. The nanocellulose is commonly subjected to dialysis treatment in

School of Chemistry and Physics, University of KwaZulu-Natal, Westville Campus, Private Bag X54001, Durban, 4000, South Africa. E-mail: vanzylw@ukzn.ac.za; Tel: +27 31 260 3188

† Electronic supplementary information (ESI) available: Preparation of nanocellulose from bacterial nanocellulose through dialysis method; set-up of copper plates in apparatus for PPy@BNCC/PVA analysis; a photograph showing the conductivity apparatus and set-up; TEM image of an active SCOBY bacteria; size distribution curves representing BNCC from dialysis-free and dialysis methods; FT-IR spectrum of dialyzed BNCC sample and for different PPy@BNCC samples including discussion; Raman spectrum of dialyzed BNCC sample; example of calculated mass, volume, and density of samples; measured current/A for PPy@BNCC/PVA from dialysis-free and dialyzed methods. See DOI: 10.1039/d0ra04649c

the final step that produces well-defined nanocrystalline cellulose (NCC) and the non-crystalline (amorphous) parts of the cellulose are removed. But the dialysis step has distinct disadvantages, including: (i) it is tremendously time-consuming and causes a huge bottleneck when compared to the other steps in the process, (ii) it requires significant volumes of water to reach neutral pH, making the overall process less environmentally friendly and raises production costs, and (iii) disposal of the residual hydrolysis acid from dialysis makes it a health and safety issue inhibiting any large scale production. The dialysis-free extraction and characterization of cellulose crystals from almond shells have been reported[26] but no dialysis-free method to produce solely NCC has been developed to date. Although NCC was not isolated, we are aware of only one study[27] in line with ours where a dialysis-free method was reported where NCC was derived from cotton, mixed with PPy and embedded in latex—the demand for a dialysis-free method of producing NCC is ongoing as a resourceful production method.

In addition to plant sources, cellulose fibers are secreted extracellularly by certain bacteria—bacterial cellulose (BC).[3,28,29] A major advantage of BC is that unlike cellulose derived from pulp sources such as trees, BC is produced directly as a native cellulose membrane that requires no further chemical treatment to remove lignin and hemicelluloses.[30] Among the acetic acid bacteria (AAB) found in Kombucha, the most efficient producer[31] of bacterial cellulose (BC) is *Gluconacetobacter xylinus* (reclassified from *Acetobacter xylinum*),[32] a Gram-negative strain of acetic acid producing bacteria.[33] Kombucha has been investigated as a novel model system for cooperativity in a complex multi-species microbial ecosystem.[34] The AAB combined with yeasts (the inoculum) have been identified as the main microorganisms during Kombucha fermentation.[35,36] In this study, we prepared BC from Kombucha tea derived from fermented sugary tea inoculated with bacteria and yeast, known as a symbiotic colony of bacteria and yeast (SCOBY).[37–39] Over the fermentation period (8–10 days) a cellulosic biofilm is formed that floats on the fermented liquid.[40] BC is secreted as a ribbon-shaped fibrils less than 100 nm wide and composed of fine 2–4 nm nanofibrils and has been used as a support in bioengineering[33,41,42] and advanced fiber composites.[43] There are a variety of benefits in using NCC for various applications due to its distinctive properties such as biocompatibility, biodegradation, high strength and specific surface area, high crystallinity index and low toxicity.[44–46]

BNCC has been prepared from side-streams of Kombucha beverages during production using mechanical processing, specifically multiple microfluidization cycles[47]—the study showed the characteristics of the fiber morphology and size formed during mechanical treatment. It is, however, very different when compared to chemical treatment where the amorphous regions are the weakest chemical link, break and get removed, significantly reducing lengths of the remaining crystalline nanocellulose. Our method relies on the chemical processing of an *in situ* generated composite formed by mixing BNCC with conducting polypyrrole (PPy) and subsequently embedded in polyvinyl alcohol (PVA) matrix, PPy@BNCC/PVA. The addition of PPy to BNCC showed good PPy dispersion, enhanced the structural integrity, increased the stability and exhibited bulk resistance.[48] Nanostructured polypyrrole, as one of the conducting polymers with exceptional intrinsic characteristics, has been effectively used as a flexible electrode material for a variety of applications, its role as an active material for supercapacitors has been reviewed.[49] Nanocellulose-mediated electroconductive self-healing hydrogels have also been prepared from a viscoelastic polyvinyl alcohol–borax (PB) gel matrix and nanostructured CNF–PPy (cellulose nanofibers–polypyrrole) complexes, exhibiting high strength, viscoelasticity, and biocompatibility toward multifunctional applications and has a conductivity in the range 1.5–4.8 S m^{-1} which linearly correlates with the amount of PPy added.[50] The use of PPy as a hydrogel for solid-state supercapacitor applications are popular investigations, for example, in the morphology-controlled fabrication of a pure polypyrrole hydrogel without cross-linkers,[51] or a hydrogel-based composite with PVA/graphene-oxide/PPy components for elastic supercapacitor applications.[52] Polypyrrole nanofiber/NiO_x composites have also been reported in a facile synthesis using a microwave method with results showing its potential application as a supercapacitor.[53]

The two most popular techniques to measure the resistivity of a material is the four-point probe method using four electric contacts pressed to the material, and the van der Pauw method[54]—which is essentially a variation of the four-point method but applied to arbitrary shaped samples. Both methods measure resistivity (Ω m) and because of the voltage–current correlation with Ohm's law it can conveniently be converted to conductivity (S m^{-1}) due to the reciprocal relationship. However, neither method eliminate contact resistance problems nor comment on the average bulk resistivity. In this study, the bulk resistivity of the PPy@BNCC/PVA material was tested with an in-house designed apparatus. The main objectives of the present study was to demonstrate the convergence of three innovative strategies, namely: (i) the fabrication of BNCC from Kombucha tea, (ii) a time-saving dialysis-free method to incorporate polymer into a composite, and (iii) a new apparatus and method to measure bulk conductivity (and resistivity).

Experimental section

Materials

Unflavored Kombucha tea under brand name Zooka, Tetley pure green tea, Hulettes white sugar, and Safari apple cider vinegar were purchased from Checkers Hyper (Westville, South Africa) and used without modification. Sulfuric acid (96% w/w) and sodium hydroxide pellets were purchased from Associated Chemical Enterprises (South Africa). Ethanol (96%), pyrrole (97%) and ferric chloride hexahydrate $FeCl_3 \cdot 6H_2O$ (98%) were purchased from Merck, polyvinyl alcohol (PVA) was purchased from VWR Chemicals. All chemicals were used as received.

Preparation of bacterial cellulose using SCOBY

The unflavored Kombucha tea (350 mL) contained a visibly grown SCOBY and was transferred from the original bottle to

a dry and sterilized 400 mL beaker and covered with an air/water permeable cloth. The small SCOBY was allowed to grow in a dark, undisturbed environment for 8–10 days. To create the cellulose growth medium, double distilled water (1 L) was boiled, then added to a 4 L sterile plastic tray. Two green tea bags were added to the boiled water and the mixture was left to brew for 15 minutes. The tea bags were removed, and 200 g white sugar was added to the solution and stirred until all the sugar dissolved. The solution was gradually cooled down to 20 °C before apple cider vinegar (150 mL) was added, followed by the SCOBY culture from the Kombucha tea at pH 5 for optimal cellulose production.[55] The dish was covered with an air/water permeable cloth and the cellulose was allowed to develop, undisturbed, in a dark environment for 3 weeks. A thick cellulose layer (biofilm) grew uniformly on the surface. The bacterial cellulose sheet was subsequently washed with deionized water and a weak bleach solution and then rinsed thoroughly with water and cut into smaller pieces. The BC pieces were rinsed in ethanol then boiled in deionized water for 40 minutes. Next, the bacterial cellulose was washed in a solution of hot 0.1 M NaOH for 20 minutes. This step was repeated up to four times, until the bacterial cellulose was white in color and all traces of tea stains removed. The bacterial cellulose was then washed thoroughly with deionized water and the pieces were ground in a blender until a paste formed, which was then stored in deionized water until further use. The total wet mass of bacterial cellulose produced was 1.188 kg, and the dry mass of bacterial cellulose produced reduced to 0.0588 kg.

Preparation of bacterial nanocellulose: dialysis-free method

The water content of the as-prepared cellulose, post washing, bleaching and mechanical blending was approximately 95.05%, based on eqn (1):

$$\text{Percentage of water content} = \frac{\text{mass of wet sample} - \text{mass of dry sample}}{\text{mass of wet sample}} \times 100 \quad (1)$$

A wet mass of 200.01 g BC (9.90 g dry bacterial cellulose) was blended and then mixed with 60% w/w sulfuric acid in a 200 mL aqueous solution using an acid : cellulose ratio of 20 mL g; it was then stirred at 40 °C for 1 hour. The hydrolysis was stopped using 400 mL double distilled H_2O, decanted, centrifuged at 9000 rpm for 10 min and washed three times. The sample was sonicated for 30 min at room temperature. For the 9.90 g of dry bacterial cellulose used, 2.96 g of dry nanocellulose was produced. The yield was calculated in triplicate to an average of 30%.

Preparation of bacterial nanocellulose: dialysis method

The PPy@BNCC composite was also prepared *via* the conventional dialysis method so that comparisons between the two methods can be made regarding conductivity measurements. From 10.20 g of bacterial cellulose produced, a mass of 2.96 g of nanocellulose was isolated following hydrolysis and dialysis. The yield was calculated in triplicate to an average of 29%. Details of the synthesis and characterization can be found in the ESI.†

In situ doping of Polypyrrole@BNCC nanocomposite

Varying ratios of pyrrole : BNCC were carried out to find the optimum conditions, as shown in Table 1. The ideal ratio was found to be 1 : 1 according to quantities in Table 2, for the synthesis of PPy@BNCC. Pyrrole monomer was added to the respective volumes of remaining hydrolysis products from BC, (containing BNCC, soluble sugars, residual acid). The mixture was gently stirred in ice-water for 1 h. Thereafter, $FeCl_3 \cdot 6H_2O$ was added into the mixture to initiate the polymerization. The polymerization proceeded in ice-water for 2 h. The obtained product was filtered and washed five times with distilled water to remove the remaining reagents.

Preparation of PPy@NCC in polyvinyl alcohol (PVA)

For the PPy@BNCC/PVA nanocomposites, 2.0 g of the prepared PPy@BNCC nanocomposite suspension was placed in 20 mL of distilled water and sonicated for 10 min to improve the

Table 1 Quantity of materials used for varying ratios of pyrrole : BNCC

Ratio pyrrole : BNCC	Volume pyrrole/mL	Mass pyrrole/g	Volume BNCC/mL	Mass BNCC/g	Mass $FeCl_3.6H_2O$/g
0 : 1	0.00	0.00	34.13	1.00	0.00
1 : 2	1.03	1.00	68.26	2.00	2.00
1 : 1	1.03	1.00	34.13	1.00	2.00
2 : 1	2.06	2.00	34.13	1.00	4.00
1 : 0	1.03	1.00	0.00	0.00	2.00

Table 2 Quantity of materials used for pyrrole : BNCC at 1 : 1 ratio

Sample	Volume pyrrole/mL	Mass pyrrole/g	Concentration BNCC/mg mL^{-1}	Mass BNCC/g	Mass $FeCl_3 \cdot 6H_2O$/g
NCC	1.03	1.00	29.30	1.00	2.00

dispersion and prevent aggregation. Separately, 2.00 g of PVA was dissolved 20 mL of distilled water, heated to 200 °C and stirred until dissolved. The sonicated PPy@BNCC nanocomposite suspension and the PVA solution were mixed together to form a homogeneous mixture and sonicated for 1 h.

Conductivity testing of the PPy@BNCC/PVA nanocomposite

For resistance testing of the PPy@BNCC/PVA composite sample, a copper plate was etched with a ferric chloride solution to create a break in circuit and was weighed, shown in Fig. S1.† An accurate volume of 0.25 mL of the prepared PPy@BNCC/PVA were filled onto the etched space with an overlap onto the copper board to ensure complete contact in the circuit. The sample plates were re-weighed. The surface area of the etched section of the plate was measured precisely using microscope software.

Resistivity test

A photograph of the conductivity measurement apparatus and set-up is shown in Fig. S2.† A DC power supply Matrix model MPS-3003L-3 was used as the power source. This was directly attached to a 217.6 Ω resistor, placed in series with the sample, and a voltmeter to measure the voltage applied in volts, and to an amp meter to measure the passing current in microamperes. By the division of the voltage by amperes, the average resistance

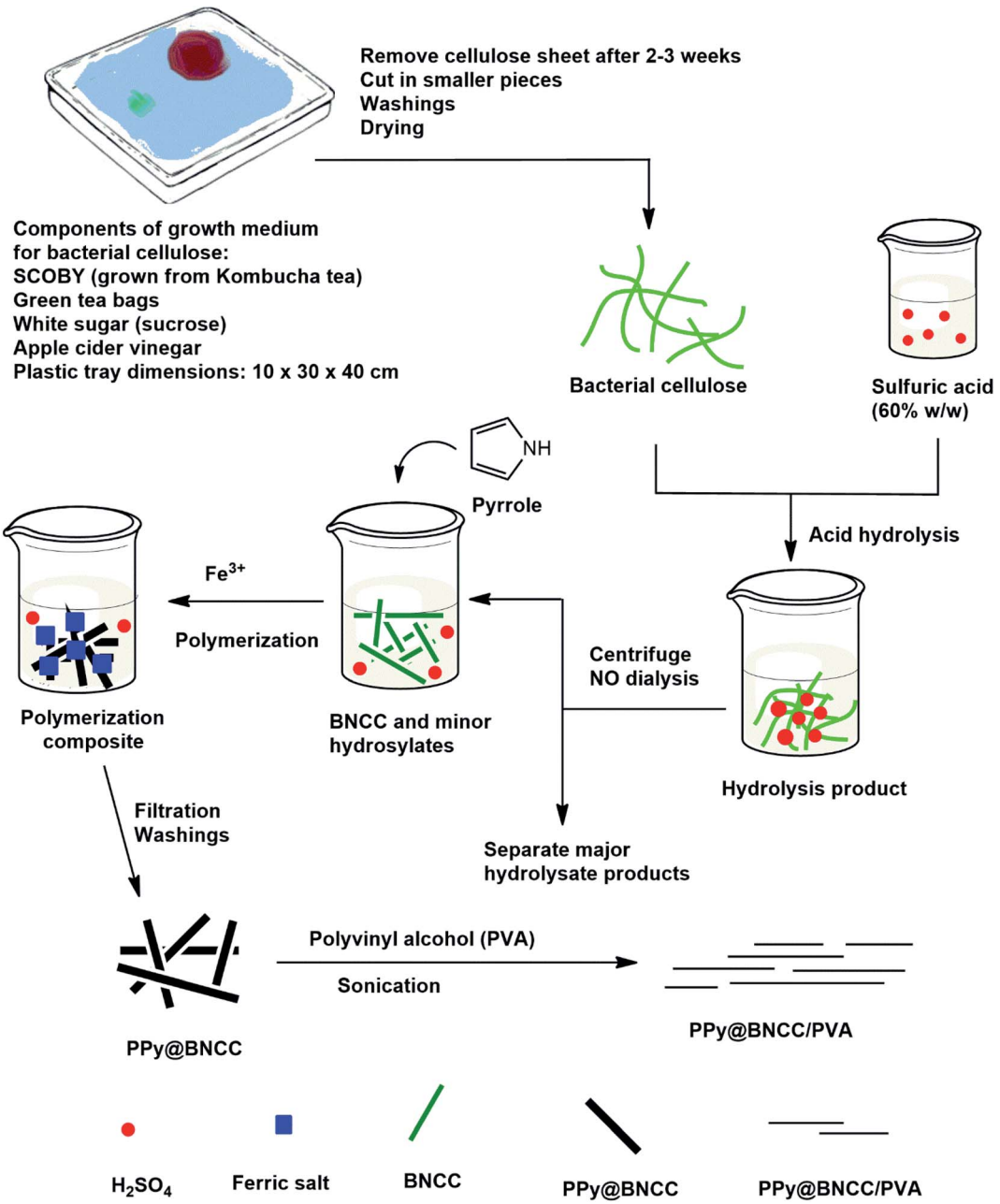

Scheme 1 Schematic representation of the dialysis-free synthetic methodology used.

was calculated, and from the reciprocal (inverse) of the resistivity (ohm meter, Ω m) the conductivity (siemens per meter, S m^{-1}) was readily obtained after appropriate unit conversion. By the plot of current *vs.* voltage, the reciprocal of the gradient is the average resistivity. The same samples used in this method was also tested using a four-point probe to confirm results and validate the system methodology.

Morphological structure analysis

The morphology for all samples were established with the aid of electron microscopy studies. For the TEM study, a JEOL-JEM 1010 (Japan) operating at 100 kV was used. TEM images for nanocellulose require a stain, thus the images were acquired using 5 μL of a 0.01 w/w% suspension of the sample deposited on a copper (Cu) TEM-grid. The deposited crystals on the TEM-grid were negatively stained after drying with 5 μL of 2 wt% uranyl acetate for 5 minutes in the dark. The dimensions of 250 randomly selected samples representing BNCC from the TEM micrographs were measured using ImageJ 1.42 software and the obtained data were processed on Origin® 9 software where the particle length, width and aspect ratio with respective standard deviation were generated. For the SEM study, a Zeiss Ultra Plus (Germany) field emission gun scanning electron microscope (FEG-SEM) was used. The samples for SEM images were deposited separately on conductive carbon tape stuck to aluminum stubs. Each sample was coated with gold with the aid of sputter coater to minimize charging. The morphology of the PPy@BNCC/PVA sample was tested prior to subjection to the conductivity tests, as well as after the testing to note any morphological change. This was accomplished using SEM Zeiss LEO 1450 (Germany), and sample images were taken directly from the Cu plate.

Spectroscopies

Fourier transform infrared (FT-IR) analyses were carried out at room temperature using a Perkin Elmer Spectrum 100 FT-IR spectrometer and was recorded in the range 380–4000 cm^{-1} at a resolution of 4 cm^{-1} fitted with an attenuated total reflectance (ATR) sampling accessory (Perkin Elmer, USA). The data was processed using Spectrum® software. A small amount of the sample was placed onto the ATR crystal and a pressure of 120 psi was applied to ensure contact between the crystal and the material. Raman spectra were measured using a Delta Nu Advantage 532 (USA) instrument fitted with a 532 nm laser source (green) and operated by NuSpec® software. Laser intensity, polarization and the integration time of the scans were varied until each sample gave clear and reproducible spectra. All analyses were carried out at room temperature with the powdered sample loaded in quartz tubes.

Results and discussion

Synthesis of bacterial cellulose

The entire synthesis methodology used in this study is outlined in Scheme 1. Significant amounts of bacterial cellulose were grown by a low-cost method from readily available household materials. Kombucha tea was used as the starting material for the growth of a symbiotic colony of bacteria and yeast (SCOBY).[37–39] We were able to produce bacterial cellulose from SCOBY by the method described, and without having to resort to strict biochemical methods such as the Hestrin–Schramm protocol.[56] In the SCOBY, the yeast component includes saccharomyces, and the bacterial component consists of *Gluconacetobacter xylinus*, which is used to oxidize yeast-produced alcohols to acetic acid.[36] Acetic acid bacterium such as *G. xylinus* can assimilate several sugars and the rod-shaped, aerobic Gram-negative bacterium secretes the extracellular polysaccharide referred to as bacterial cellulose.[57] Interestingly, we were able to capture a TEM image of an active bacteria, presumably *G. xylinus* since it predominates in this growth medium, see Fig. S3.† The BC produced by the SCOBY has remarkable mechanical properties even though it contains >95% water prior to drying.[58] In this study, the bulk of the growth medium was a broth of green tea which is typically used

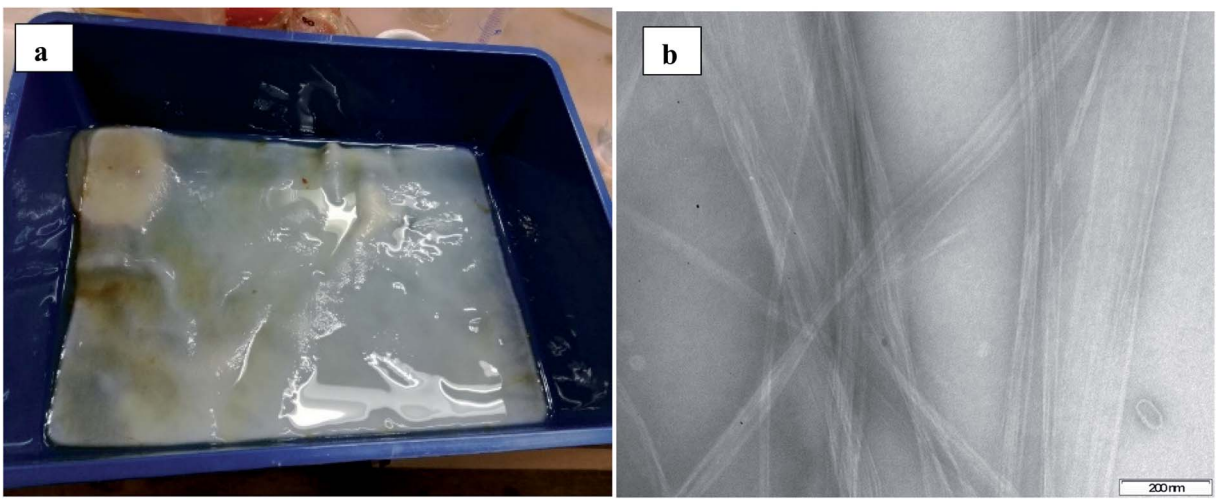

Fig. 1 (a) Bacterial cellulose film formed in growth medium after 2 weeks of growth, (b) TEM image of isolated bacterial cellulose.

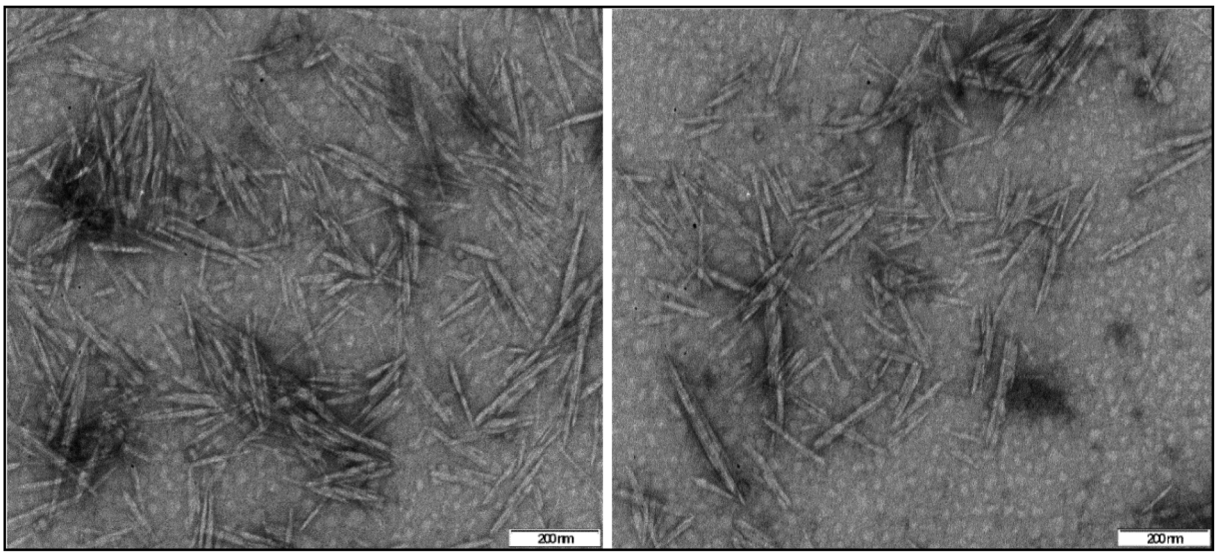

Fig. 2 TEM images of negatively stained BNCC crystalline needles prepared by the dialysis-free method.

as the fermentation medium of Kombucha tea,[55] and controlled at pH 5 with apple cider vinegar for optimal cellulose production.[59] The cost-effective carbon source was white sugar (sucrose) which is the most important component as this fuels the bacteria, it also suggests that the amount of cellulose that can be grown is virtually limitless as it only relies on the amount of added sugar and ensuring the SCOBY remains alive.[43] All these components contained some micronutrients to support growth, reproduction and functionality of the microorganisms. The growth of the cellulose showed uniformity that could be manipulated by the shape of the container. Significantly, the growth of bacterial cellulose is a bottom-up synthesis method whereby the BC is formed from the molecular level in solution, as opposed to a top-down approach which is used in the breakdown of wood pulp to form cellulose in a traditional manner, leading to waste products.

The BC has a dense surface on the air-exposed side, and a gelatinous layer on the aqueous exposed side.[60] Fig. 1(a) shows the bacterial cellulose biofilm formed after 2 weeks of growth, note the SCOBY in the top left corner that continuously biosynthesize cellulose as long as it has sufficient sugar to feed on, Fig. 1(b) shows a TEM image of uniform isolated bacterial cellulose.

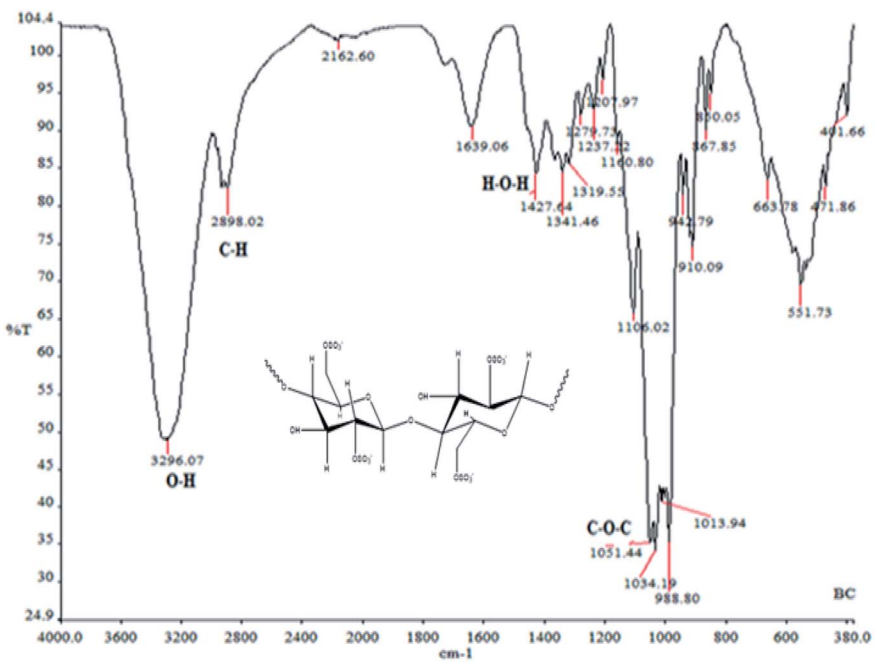

Fig. 3 FT-IR spectrum of the BNCC sample prepared by the dialysis-free method.

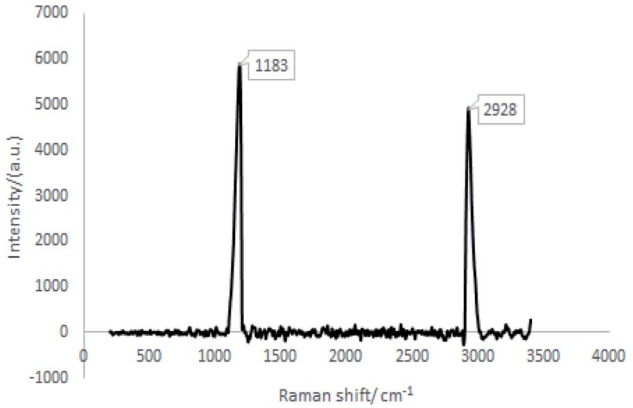

Fig. 4 Raman spectrum of BNCC from the dialysis-free method.

In bacterial cellulose the cellulase is a multicomponent enzyme which hydrolyze cellulose into smaller fragments, oligosaccharides, cellobiose or glucose, depending on a variety of parameters, and the process starts with the cleavage of the amorphous regions of the long cellulose microfibrils and give rise to several fractions of hydrolysis products.[61] The crystalline regions of cellulose are more resistant to hydrolysis due to the presence of strong hydrogen bonding when compared to the poorly aligned and less compacted amorphous regions.[62] Bacterial cellulose and nanocellulose derivatives show remarkable mechanical properties, purity and straightforward production, which has gained much interest over the years. Here, the acid catalyzed hydrolysis of the bulk fibers was carried out and the average concentration of bacterial nanocrystalline cellulose (BNCC) dialysis-free was 29.30 mg mL^{-1}.

TEM studies

TEM was used to investigate the microstructures of the produced nanocellulose, shown in Fig. 2. The BNCC has distinct needle-like shapes with calculated mean length of 130.00 ± 30.99 nm with a width of 15.00 ± 3.05 nm and aspect ratio of 9.03 ± 3.38 from 250 randomly selected nanocrystals. The high standard deviation of the dimensions suggests that the nanofibers were polydispersed as determined by the average size distributions, see Fig. S4† (dialysis-free) and Fig. S5† (dialysis). The dimensions nevertheless correlate well with NCC isolated from waste products[63] and natural hardwood pulp[64]—the ideal aspect ratio required for good stress transfer within the interaction between fibers and matrix to provide strong reinforcement and mechanical stability when included in a polymer composite is 10, and the aspect ratio of the bacterial nanocrystals reported here lie close to the ideal stress transfer minimum.[65]

FT-IR and Raman spectroscopy studies

The FT-IR spectrum from the BNCC produced by the dialysis-free method showed a broad band at 3296 cm^{-1} assigned to the O–H bend for the BNCC. A medium band at 2898 cm^{-1} of the C–H asymmetrical stretch was assigned to bacterial cellulose. The band found at 1639 cm^{-1} is associated with the bending of the absorbed water moisture for bacterial cellulose. The broad band at 1034 cm^{-1} was attributed to the pyranose backbone, Fig. 3. All peaks for nanocellulose were consistent with reported values in the region assigned (ν/cm^{-1}) as: 3320 (O–H), 2900 (C–H asym), 1646 (H–O–H bend), 1437 (CH_2 symm), 1371 (C–H asym bend), 1018 (C–O–C) and 898 (C–H deform) modes of the β-glycosidic linkage between the anhydroglucose rings.[63] These results were consistent with the cellulose structure which suggests that the method of growing pure cellulose as well as the production and isolation of nanocellulose from bacterial cellulose was successfully demonstrated.

The corresponding FT-IR spectrum of the dialyzed sample is shown in Fig. S6.† Additionally, the FT-IR spectra for (i) neat polypyrrole, and composites (ii) PPy@BNCC (dialysis method) and (iii) PPy@BNCC (dialysis-free method) are shown in Fig. S7.†

Raman spectroscopy was performed on the dialysis-free BNCC nanocomposite and showed characteristic Raman shifts for cellulose, see Fig. 4.[66] The corresponding Raman spectrum of the dialyzed sample is shown in Fig. S8.†

Synthesis of PPy@BNCC nanocomposite

Cellulose fibers were hydrolyzed by sulfuric acid (60% w/w) yielding a hydrolysis product consisting of nanocellulose,

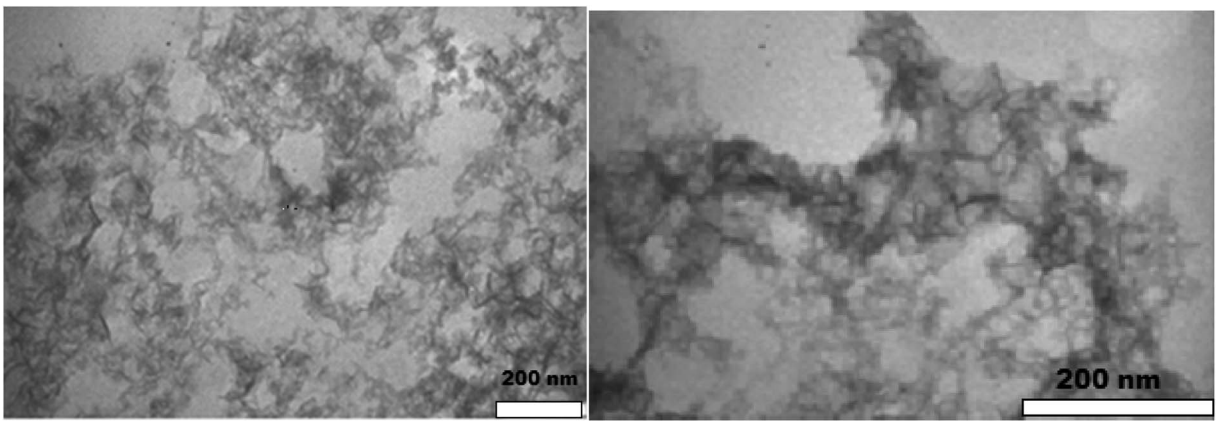

Fig. 5 TEM images of PPy@BNCC prepared by dialysis-free method.

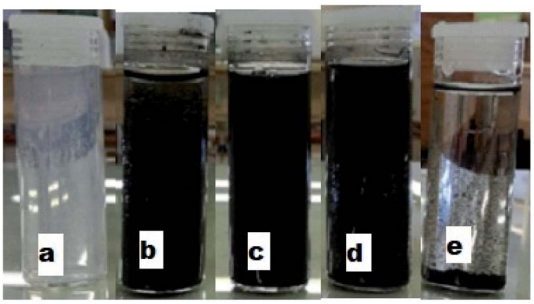

Fig. 6 Digital pictures of varying ratios of PPy : BNCC (L–R): (a) 0 : 1; (b) 1 : 2; (c) 1 : 1; (d) 2 : 1 and (e) 1 : 0, when left for 30 minutes.

soluble sugars, and residual acid. The dialysis-free BNCC had no significant effect on the polymerization of pyrrole. The polymerization of pyrrole monomer was initiated with $FeCl_3 \cdot 6H_2O$ added to the hydrolysis product, and the generated PPy was deposited on the nanocellulose, yielding a black precipitate of the PPy@BNCC nanohybrid that was easily separated from the polymerization product by filtration and washing, and finally dried, yielding a powder.

TEM studies of nanocomposite microstructures

TEM was used to investigate the microstructures of pure polypyrrole and the prepared PPy@BNCC nanocomposites. The polymerization of the pyrrole monomer without BNCC was found to have an aggregated nodular structure whilst for PPy@BNCC there was a well-defined continuous network and the dispersal of the BNCC within the nanocomposite was visible, Fig. 5. The hydrogen bonds between imine groups of PPy and hydroxyl groups of nanocellulose presumably cause a strong interaction to assist with the growing of the continuous nanosheath of PPy on BNCC and prevented the formation of PPy aggregation. Large scale aggregation of PPy was not observed which demonstrated that nanocellulose acted as a suitable template for the polymerization of pyrrole monomer.

Synthesis of PPy@BNCC combined with PVA: suspension studies

Before the synthesis of PPy@BNCC combined with PVA could commence, a sense of the compatibility between PPy and BNCC had to be established. This was done by determining the most suitable suspension characteristics of PPy to BNCC in five different ratios by weight for (a) 0 : 1, (b) 1 : 2, (c) 1 : 1, (d) 2 : 1 and (e) 1 : 0, shown in Fig. 6. The solution was white and opaque as expected for BNCC (0 : 1), with excellent suspension and no separation. The PPy : BNCC in a 1 : 2 ratio showed that after 20 minutes the polypyrrole was well dispersed but after 30 minutes the excess BNCC slowly began to separate from the polypyrrole, and the denser polypyrrole settled to the bottom. When this ratio was dispersed in PVA, the sample did not dry evenly because the PPy was unevenly distributed in the film. The ratio of 1 : 1 proved to be most suitable where the PPy was well dispersed. After 30 minutes there was no change in the consistency and the composite remained well dispersed in the suspension. When dried in PVA, the sample dried evenly into a smooth film that was easily removed from the Petri dish. It was flexible and maintained its structural integrity. Similar results were seen for ratio 2 : 1, but over hours the suspension separated slightly due to the higher amount of PPy and unfortunately, when dried in PVA, the film became hard, brittle and did not set in a neat film. For the 1 : 0 ratio, no BNCC was used and the PPy settled to the bottom of the vial instantly. When drying in PVA, there was no homogeneity and the polypyrrole aggregated with a rough texture and no connected network. Therefore, the 1 : 1 ratio proved ideal to bring out optimal mechanical properties (strong enough to retain structural integrity yet sufficiently flexible when bent without shattering) and electrical properties to perform conductivity measurement. The mass yield obtained for PPy@BNCC was 0.812 g following the optimum ratio. The dialysis-free process of producing BNCC presents a facile, inexpensive, and eco-friendly synthesis of PPy@BNCC type nanocomposites.

Synthesis of PPy@BNCC combined with PVA

To evaluate the feasibility of PPy@BNCC as a conductive polymer nanocomposite suitable for use in our apparatus, it had to be formed into a flexible and moldable material that does not interfere with the electrical properties of the overall composite and we found this was best achieved through mixing with polyvinyl alcohol (PVA). To achieve higher conductivity at the same PPy content, it was expected that all the PPy participate in the fabrication of a continuously conductive network in the PVA

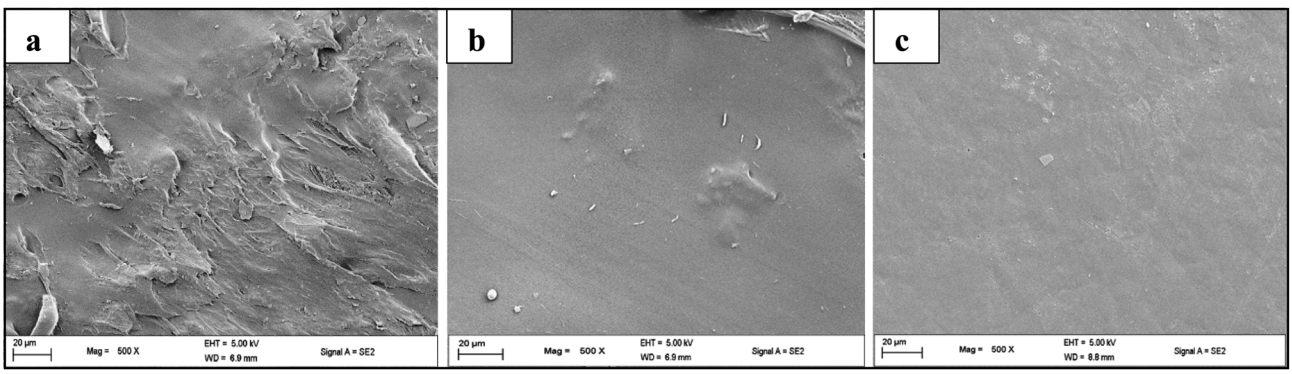

Fig. 7 SEM image of (a) PPy in PVA, (b) and (c) dialysis-free method of PPy@BNCC/PVA.

matrix. Neat PPy caused agglomeration due to poor suspension stability (Fig. 6(e)) that made the formation of conductive networks difficult, see Fig. 7(a). However, a continuous network structure of PPy@BNCC nanocomposite was formed by incorporation of BNCC due to the improved stability in PVA. The PPy@BNCC nanocomposite was found in the interstitial space between the PVA and formed a continuous network which benefitted from the good suspension property and high aspect ratio of the PPy@BNCC nanocomposite. The nanocomposite had a smooth surface texture, good homogeneity and an improved connected network. The PPy@BNCC/PVA nanocomposite prepared by the dialysis-free method is shown in Fig. 7(b and c). The facile, cost-efficient, time saving and scalable approach to PPy@BNCC/PVA nanocomposites opens new research avenues to consider for the large-scale application of these and related NCC-based conductive nanocomposites.

Electrical properties: resistivity and conductivity

We have developed an in-house apparatus capable of measuring the bulk resistivity of a polymer-based nanocomposite in a controlled environment. The reason for our design concept is due to the conventional four-point probe measurement method that has a number of drawbacks, Heaney listed at least ten,[67] including the difficulty in securing good electric contact is made to the sample surface in a consistent and reproducible manner. The conductivity measurements performed in this study were done on three separate types of samples, namely: (i) PPy@BNCC/PVA prepared by the dialysis-free method, (ii) PPy@BNCC/PVA prepared by the dialysis method and (iii) for comparison reasons and to validate our results, testing with the four-point measurement technique. To accurately determine the conductivity of the prepared films, it was necessary to first derive key dimensions, starting with the film thickness: firstly, the density of each PPy@BNCC/PVA composite was determined by calculating the volume of water present. By weighing the wet sample on the copper plate and then subtracting the weight of the sample, the mass of water could be calculated with the known density of water at room temperature. An example of calculated details for determining the mass, volume, and density of samples are shown in Table S1.† The volume of the PPy@BNCC/PVA nanocomposite could be obtained by subtracting the volume of water from the volume used (0.25 mL). The dry PPy@BNCC/PVA nanocomposite weight divided by the volume yielded the density of each sample. The thickness of the film could be calculated from eqn (2)–(4):

$$\text{Volume} = (\text{length} \times \text{breadth}) \times \text{thickness} \quad (2)$$

$$\text{Volume} = (\text{surface area}) \times \text{thickness} \quad (3)$$

$$\text{Thickness/mm} = \frac{\text{volume/mm}^3}{\text{surface area/mm}^2} \quad (4)$$

The volume of dried PPy@BNCC/PVA nanocomposite divided by the surface area of the sample on the copper plate yielded the thickness of the film which was 0.573 and 0.599 mm for the dialysis-free and dialysis methods, respectively.

The volume resistivity was determined with eqn (5):

$$\rho = \frac{\text{surface area}}{\text{thickness}} \times \text{resistance} \quad (5)$$

Using this thickness, calculated in eqn (5), multiplied by the film width, the surface area of the side of the film was measured, eqn (5) can be re-written as (6):

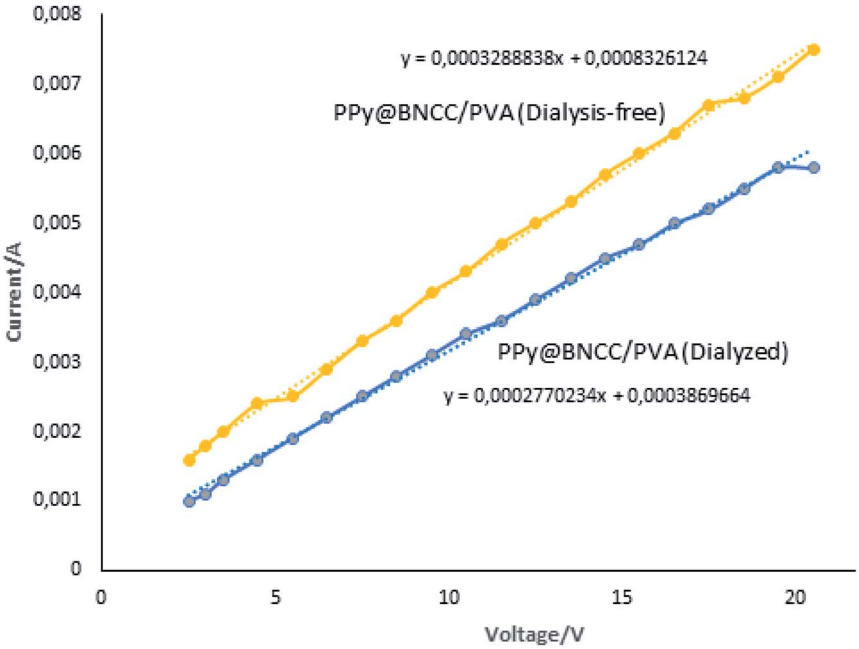

Fig. 8 Linear relationship based on Ohm's law showing the change in current as voltage was applied for dialysis-free *vs.* dialyzed samples.

$$\rho = \frac{(\text{thickness}) \times (\text{width})}{\text{length}} \times \text{resistance} \quad (6)$$

and thus eqn (7) gives the volume resistivity as:

$$\rho = \frac{\text{surface area of the side}}{\text{length}} \times \text{resistance} \quad (7)$$

As expected, samples without polypyrrole showed no measurable conducting properties. For ratio 1 : 1, which we found to be the best suited ratio, the composite was found to have the lowest resistivity (highest conductivity). The resistance can be determined from the reciprocal of the gradient from the current *vs.* voltage graphs, but the resistivity per mm can also be compared to the calculated resistivity per mm. We compared the PPy@BNCC/PVA dialysis-free composite with the dialyzed sample, and interestingly, the dialysis-free composite showed higher conductivity, see Fig. 8.

The conductance of the synthesized dialysis-free PPy@BNCC/PVA nanocellulose was larger than samples subjected to dialysis and we propose this was due to the dialysis-free material that contained residual hydrolyzed sulfuric acid components that can act as doping agents for PPy, endowing the nanocomposite with improved electrical conductivity. Table 3 shows the main electrical properties measured including resistivity, conductivity, average resistance and comparison with the four-point measurement.

Table 3 The resistivity and conductivity calculations per unit length (mm and m) for PPy@BNCC/PVA nanocomposite following dialyzed and dialysis-free synthetic protocols

Procedure	Dialyzed	Dialysis-free
Average calculated resistance (Ω)[a]	3091.47	2339.94
Standard deviation	266.52	360.22
Variance	71 035.38	129 758.25
Thickness/mm	0.61	0.60
Width of sample/mm	21.62	21.17
Surface area of the side/mm^2	13.19	12.70
Length of sample/mm	11.75	11.90
Resistivity calculated (Ω mm)	3469.87	2495.48
Resistivity calculated (Ω m)	3.47	2.50
Conductivity calculated (S mm^{-1})	2.88×10^{-4}	4.00×10^{-4}
Conductivity calculated (S m^{-1})	2.88×10^{-1}	4.00×10^{-1}
Resistance from line of best fit $\left(\frac{1}{\text{gradient}}\right)$	3609.81	3040.59
Resistivity from line of best fit (Ω mm)	2928.07	2341.21
Resistivity from line of best fit (Ω m)	2.93	2.34
Conductivity from line of best fit (S mm^{-1})	3.41×10^{-4}	4.27×10^{-4}
Conductivity from line of best fit (S m^{-1})	3.41×10^{-1}	4.27×10^{-1}
Four-point probe resistivity (Ω m)	2.90	2.31
Four-point probe conductivity (S m^{-1})	3.49×10^{-1}	4.33×10^{-1}

[a] See Tables S2 and S3 for calculations of measured current at applied voltage.

The values for the calculated resistivity are close to the values obtained from the line of best fit for the average resistance. For the dialysis-free PPy@BNCC/PVA nanocomposite, the calculated average volume resistivity was calculated at 2495.48 Ω mm (4.00×10^{-4} S mm^{-1}) with the corresponding volume resistivity obtained from the line of best fit at 2341.21 Ω mm (4.27×10^{-4} S mm^{-1}). The nearest reported composite to this study consists of PPy and CNC (derived from cotton fibers) using natural rubber as a matrix which recorded a best case conductivity response lower than ours at 1.22×10^{-3} S m^{-1}, measured on undeformed dialysis-free samples through a two-point apparatus.[27] For the dialyzed sample the calculated average volume resistivity was calculated at 3469.87 Ω mm (2.88×10^{-4} S mm^{-1}) with the corresponding volume resistivity obtained from the line of best fit at 2928.07 Ω mm (3.41×10^{-4} S mm^{-1}). The results demonstrated conclusively that the average conductivity for PPy@BNCC/PVA made from dialysis-free bacterial nanocellulose is higher when compared to the dialyzed method.

At present we have no definitive explanation for this observation, but since no attempt was made to neutralize the dialysis-free samples from residual sulfate group components (sulfates and related species) attached to the cellulose surface, we suggest these groups could act as doping agents toward the conducting PPy and promote an improvement of the overall composite conductivity. The results obtained by using a simple ammeter and voltmeter gave outstanding results. When repeat experiments were performed and compared using a traditional four-point probe measurement, the results were a close match. Our apparatus proved to provide an excellent alternate route to the four-point probe method for resistivity/conductivity measurements.

This work shows that by capitalizing on the physiognomies of nanocellulose not subjected to dialysis, unique traits can be further developed as an advantage for useful applications. We demonstrate that avoiding the laborious dialysis step is not necessarily a disadvantage but could be exploited by combining the material with other components that could in fact contribute in amplifying existing properties. In this work, this enhancement benefitted from the good dispersion and high aspect ratio of the nanocomposite to produce a more cost effective, environmentally friendly process.

Conclusions

This work demonstrated that three overlapping strategies, namely: (i) the fabrication of BNCC from Kombucha tea, (ii) the avoidance of a time-consuming dialysis step, and (iii) the design and workability of an apparatus to measure bulk resistivity, could all be incorporated and aided into one synthesis methodology to enhance and exploit properties already present in the material in a cost effective and sustainable manner.

The extraction of nanocellulose from bacterial cellulose derived from Kombucha tea and its explicit use in materials science is rare. The obtained BNCC was successfully hydrolyzed with sulfuric acid, and the nanocrystal dimensions compared

favorably with those derived from conventional dialyzed nanocrystals, and we propose the dialysis-free method should become a more popular strategy in the formation of BNCC/polymer composites. The PVA served as an excellent medium to facilitate the nanocomposite in a well dispersed form. The results showed that the polypyrrole : BNCC ratio of 1 : 1 was ideal to retain structural integrity and optimum conductivity of the nanocomposite. By comparing the electrical properties of the dialysis-free *vs.* dialyzed samples containing the same components, we were able to demonstrate the PPy@BNCC/PVA sample prepared by the dialysis-free method showed improved conductivity.

The traditional means to determine electrical conductivity is the four-point probe technique and it has proven disadvantages. In this study, we overcame that obstacle by designing an apparatus where the entire sample comes in contact with a copper plate with a voltage drop applied across the sample whilst a variable current flow is applied which allows for accurate bulk resistance (and thus conductance) measurements; to obtain a similar result with the four-point probe is to take the average of numerous measurements. We also demonstrated this expedient method gave results that was confirmed with the traditional four-point probe method and the favorable results were validated. A facile, reproducible, sustainable, cost-effective, and scalable approach to prepare a cellulose-based nanocomposite was achieved *via* a dialysis-free and *in situ* doping strategy.

Abbreviations

BNCC	Bacterial nanocrystalline cellulose
BC	Bacterial cellulose
NC	Nanocellulose
PPy	Polypyrrole
PVA	polyvinyl alcohol

Conflicts of interest

The authors declare no competing financial interest.

Acknowledgements

The authors acknowledge the University of KwaZulu-Natal, the National Research Foundation (South Africa) and the Eskom TESP grant for financial support.

References

1 D. Klemm, B. Heublein, H.-P. Fink and A. Bohn, Cellulose: Fascinating Biopolymer and Sustainable Raw Material, *Angew. Chem., Int. Ed.*, 2005, **44**, 3358–3393, DOI: 10.1002/anie.200460587.

2 H. Shaghaleh, X. Xu and S. Wang, Current progress in production of biopolymeric materials based on cellulose, cellulose nanofibers, and cellulose derivatives, *RSC Adv.*, 2018, **8**, 825–842, DOI: 10.1039/c7ra11157f.

3 J. Wang, J. Tavakoli and Y. Tang, Bacterial cellulose production, properties and applications with different culture methods – A review, *Carbohydr. Polym.*, 2019, **219**, 63–76, DOI: 10.1016/j.carbpol.2019.05.008.

4 A. Dufresne, Nanocellulose: a new ageless bionanomaterial, *Mater. Today*, 2013, **16**, 220–227, DOI: 10.1016/j.mattod.2013.06.004.

5 Y. Habibi, L. A. Lucia and O. J. Rojas, Cellulose nanocrystals: chemistry, self-assembly, and applications, *Chem. Rev.*, 2010, **110**, 3479–3500, DOI: 10.1021/cr900339w.

6 D. Klemm, F. Kramer, S. Moritz, T. Lindstrom, M. Ankerfors, D. Gray and A. Dorris, Nanocelluloses: A New Family of Nature-Based Materials, *Angew. Chem., Int. Ed.*, 2011, **50**, 5438–5466, DOI: 10.1002/anie.201001273.

7 L. T. Fan, M. M. Gharpuray and Y. H. Lee, Acid hydrolysis of cellulose, in *Cellulose Hydrolysis, Biotechnology monographs*, 1987, Springer, Berlin, Heidelberg, vol. 3, pp. 121–148. DOI: 10.1007/978-3-642-72575-3_4.

8 C. J. Chirayil, L. Mathew and S. Thomas, Review of recent research in nano cellulose preparation from different lignocellulosic fibers, *Rev. Adv. Mater. Sci.*, 2014, **37**, 20–28, DOI: 10.2991/icmemtc-16.2016.148.

9 H. Charreau, M. L. Foresti and A. Vázquez, Nanocellulose patents trends: a comprehensive review on patents on cellulose nanocrystals, microfibrillated and bacterial cellulose, *Recent Pat. Nanotechnol.*, 2013, **7**, 56–80, DOI: 10.2174/18722105130106.

10 D. Klemm, E. D. Cranston, D. Fischer, M. Gama, S. A. Kedzior, D. Kralisch, F. Kramer, T. Kondo, T. Lindström, S. Nietzsche, K. Petzold-Welcke and F. Rauchfuß, Nanocellulose as a natural source for groundbreaking applications in materials science: Today's state, *Mater. Today*, 2018, **21**, 720–746, DOI: 10.1016/j.mattod.2018.02.001.

11 R. J. Moon, A. Martini, J. Nairn, J. Simonsen and J. Youngblood, Cellulose Nanomaterials Review: Structure, Properties and Nanocomposites, *Chem. Soc. Rev.*, 2011, **40**, 3941–3994, DOI: 10.1039/C0CS00108B.

12 M. Mariano, N. El Kissi and A. Dufresne, Nanocrystalline cellulose and Related Nanocomposites: Review of Some Properties and Challenges, *J. Polym. Sci., Part B: Polym. Phys.*, 2014, **52**, 791–806, DOI: 10.1002/polb.23490.

13 N. Mahfoudhi and S. Boufi, Nanocellulose as a novel nanostructured adsorbent for environmental remediation: a review, *Cellulose*, 2017, **24**, 1171–1197, DOI: 10.1007/s10570-017-1194-0.

14 K. J. De France, T. Hoare and E. D. Cranston, Review of Hydrogels and Aerogels Containing Nanocellulose, *Chem. Mater.*, 2017, **29**, 4609–4631, DOI: 10.1021/acs.chemmater.7b00531.

15 S. A. Ogundare and W. E. van Zyl, A review of cellulose-based substrates for SERS: fundamentals, design principles, applications, *Cellulose*, 2019, **26**, 6489–6528, DOI: 10.1007/s10570-019-02580-0.

16 Y. Habibi, Key Advances in the Chemical Modification of Nanocelluloses, *Chem. Soc. Rev.*, 2014, **43**, 1519–1542, DOI: 10.1039/C3CS60204D.
17 S. Eyley and W. Thielemans, Surface modification of cellulose nanocrystals, *Nanoscale*, 2014, **6**, 7764–7779, DOI: 10.1039/c4nr01756k.
18 G. Chinga-Carrasco, Potential and Limitations of Nanocelluloses as Components in Biocomposite Inks for Three-Dimensional Bioprinting and for Biomedical Devices, *Biomacromolecules*, 2018, **19**, 701–711, DOI: 10.1021/acs.biomac.8b00053.
19 J. A. Kelly, M. A. Giese, K. E. Shopsowitz, W. Y. Hamad and M. J. MacLachlan, The Development of Chiral Nematic Mesoporous Materials, *Acc. Chem. Res.*, 2014, **47**, 1088–1096, DOI: 10.1021/ar400243m.
20 M. Jorfi and E. J. Foster, Recent Advances in Nanocellulose for Biomedical Applications, *J. Appl. Polym. Sci.*, 2015, **132**, 41719–41737, DOI: 10.1002/app.41719.
21 M. Roman, Toxicity of Cellulose Nanocrystals: A Review, *Ind. Biotechnol.*, 2015, **11**, 25–33, DOI: 10.1089/ind.2014.0024.
22 R. M. Domingues, M. E. Gomes and R. L. Reis, The Potential of Nanocrystalline cellulose in Tissue Engineering Strategies, *Biomacromolecules*, 2014, **15**, 2327–2346, DOI: 10.1021/bm500524s.
23 J. M. Dugan, J. E. Gough and S. J. Eichhorn, Bacterial Cellulose Scaffolds and Cellulose Nanowhiskers for Tissue Engineering, *Nanomedicine*, 2013, **8**, 287–298, DOI: 10.2217/nnm.12.211.
24 N. Lin and A. Dufresne, Nanocellulose in Biomedicine: Current Status and Future Prospect, *Eur. Polym. J.*, 2014, **59**, 302–325, DOI: 10.1016/j.eurpolymj.2014.07.025.
25 A. Mandal and D. Chakrabarty, Isolation of nanocellulose from waste sugarcane bagasse (SCB) and its characterization, *Carbohydr. Polym.*, 2011, **86**, 1291–1299, DOI: 10.1016/j.carbpol.2011.06.030.
26 N. Maaloul, R. B. Arfi, M. Rendueles, A. Ghorbal and M. Diaz, Dialysis-free extraction and characterization of cellulose crystals from almond (Prunus dulcis) shells, *J. Mater. Environ. Sci.*, 2017, **8**, 4171–4181.
27 X. Zhang, X. Wu, C. Lu and Z. Zhouhang, Dialysis-free and *in situ* doping synthesis of polypyrrole@cellulose nanowhiskers nanohybrid for preparation of conductive nanocomposites with enhanced properties, *ACS Sustainable Chem. Eng.*, 2015, **3**, 675–682, DOI: 10.1021/sc500853m.
28 H. El-Saied, A. H. Basta and R. H. Gobran, Research progress in friendly environmental technology for the production of cellulose products (bacterial cellulose and its application), *Polym.-Plast. Technol. Eng.*, 2004, **43**, 797–820, DOI: 10.1081/PPT-120038065.
29 M. H. Deinema and L. Zevenhuizen, Formation of cellulose fibrils by Gram-negative bacteria and their role in bacterial flocculation, *Arch. Mikrobiol.*, 1971, **78**, 42–57, DOI: 10.1007/BF00409087.
30 M. Gama, F. Dourado and S. Bielecki, Bacterial Nanocellulose, in *From Biotechnology to Bio-Economy*, Elsevier, 1st edn, 2016.
31 J. L. Strap, A. Latos, I. Shim and D. T. Bonetta, Characterization of pellicle inhibition in Gluconacetobacter xylinus 53582 by a small molecule, pellicin, identified by a chemical genetics screen, *PLoS One*, 2011, **6**, e28015, DOI: 10.1371/journal.pone.002801532.
32 Y. Yamada, P. Yukphan, T. L. V. Huong, Y. Muramatsu, D. Ochaikul, D. S. Tanasupawat and Y. Nakagawa, Description of Komagataeibacter gen. nov., with proposals of new combinations (Acetobacteraceae), *J. Gen. Appl. Microbiol.*, 2012, **58**, 397e404, DOI: 10.2323/jgam.58.397.
33 M. Iguchi, S. Yamanaka and A. Budhiono, Bacterial cellulose—a masterpiece of nature's arts, *J. Mater. Sci.*, 2000, **35**, 261–270, DOI: 10.1023/A:1004775229149.
34 A. May, S. Narayanan, J. Alcock, A. Varsani, C. Maley and A. Aktipis, Kombucha: a novel model system for cooperation and conflict in a complex multi-species microbial ecosystem, *PeerJ*, 2019, **7**, e7565, DOI: 10.7717/peerj.756534.
35 S. A. V. Soto, S. Beaufort, J. Bouajila, J.-P. Souchard and P. Taillandier, Understanding Kombucha Tea Fermentation: A Review, *J. Food Sci.*, 2018, **83**, 580–588.
36 F. De Filippis, A. D. Troise, P. Vitaglione and D. Ercolini, Different temperatures select distinctive acetic acid bacteria species and promotes organic acids production during Kombucha tea fermentation, *Food Microbiol.*, 2018, **73**, 11–16, DOI: 10.1016/j.fm.2018.01.008.
37 N. O. Kozyrovska, O. M. Reva and V. B. Goginyan, Kombucha microbiome as a probiotic: a view from the perspective of post-genomics and synthetic ecology, *Biopolym. Cell*, 2012, **28**, 103–113, DOI: 10.7124/bc.000034.
38 G. Sreeramulu, Y. Zhu and W. Knol, Kombucha fermentation and its antimicrobial activity, *J. Agric. Food Chem.*, 2000, **48**, 2589e2594, DOI: 10.1021/jf991333m.
39 P. Aduri, K. A. Rao, A. Fatima, P. Kaul and A. Shalini, Study of biodegradable packaging material produced from SCOBY, *Res. J. Life Sci., Bioinf., Pharm. Chem. Sci.*, 2019, **5**, 389–404, DOI: 10.26479/2019.0503.32.
40 C. Sharma and N. K. Bhardwaj, Biotransformation of fermented black tea into bacterial nanocellulose *via* symbiotic interplay of microorganisms, *Int. J. Biol. Macromol.*, 2019, **132**, 166–177, DOI: 10.1016/j.ijbiomac.2019.03.202.
41 R. F. Jonas and L. F. Farah, Production and application of microbial cellulose, *Polym. Degrad. Stab.*, 1998, **59**, 101–106, DOI: 10.1016/S0141-3910(97)00197-3.
42 E. E. Brown and M.-P. G. Laborie, Bioengineering bacterial cellulose/poly (ethylene oxide) nanocomposites, *Biomacromolecules*, 2007, **8**, 3074–3081, DOI: 10.1021/bm700448x.
43 K. Y. Lee, G. Buldum, A. Mantalaris and A. Bismarck, More Than Meets the Eye in Bacterial Cellulose: Biosynthesis, Bioprocessing, and Applications in Advanced Fiber Composites, *Macromol. Biosci.*, 2014, **14**, 10–32, DOI: 10.1002/mabi.201300298.
44 I. Siró and D. Plackett, Microfibrillated cellulose and new nanocomposite materials: a review, *Cellulose*, 2010, **17**, 459–494, DOI: 10.1007/s10570-010-9405-y.

45 J. Cowie, E. M. Bilek, T. H. Wegner and J. Shatkin, Market projections of cellulose nanomaterial-enabled products, *Tappi J.*, 2014, **13**, 57–69, DOI: 10.32964/TJ13.6.57.

46 N. Lin, J. Huang and A. Dufresne, Preparation, properties and applications of polysaccharide nanocrystals in advanced functional nanomaterials: a review, *Nanoscale*, 2012, **4**, 3274–3294, DOI: 10.1039/C2NR30260H.

47 S.-O. Dima, D.-M. Panaitescu, C. Orban, M. Ghiurea, S.-M. Doncea, R. C. Fierascu, C. L. Nistor, E. Alexandrescu, C.-A. Nicolae, B. Trica, A. Moraru and F. Oancea, Bacterial Nanocellulose from Side-Streams of Kombucha Beverages Production: Preparation and Physical-Chemical Properties, *Polymers*, 2017, **9**, 374, DOI: 10.3390/polym9080374.

48 S. Srivastav, P. Tammela, D. Brandell and M. Sjödin, Understanding ionic transport in polypyrrole/nanocellulose composite energy storage devices, *Electrochim. Acta*, 2015, **182**, 1145–1152, DOI: 10.1016/j.electacta.2015.09.084.

49 Y. Huang, H. Li, Z. Wang, M. Zhu, Z. Pei, Q. Xue, Y. Huang and C. Zhi, Nanostructured Polypyrrole as a flexible electrode material of supercapacitor, *Nano Energy*, 2016, **22**, 422–438, DOI: 10.1016/j.nanoen.2016.02.047.

50 Q. Ding, X. Xu, Y. Yue, C. Mei, C. Huang, S. Jiang, Q. Wu and J. Han, Nanocellulose-Mediated Electroconductive Self-Healing Hydrogels with High Strength, Plasticity, Viscoelasticity, Stretchability, and Biocompatibility toward Multifunctional Applications, *ACS Appl. Mater. Interfaces*, 2018, **10**, 27987–28002, DOI: 10.1021/acsami.8b09656.

51 J. Bo, X. Luo, H. Huang, L. Li, W. Lai and X. Yu, Morphology-controlled fabrication of polypyrrole hydrogel for solid-state supercapacitor, *J. Power Sources*, 2018, **408**, 105–111, DOI: 10.1016/j.jpowsour.2018.10.064.

52 D. Wei, J. Zhu, L. Luo, H. Huang, L. Li and X. Yu, Fabrication of poly(vinyl alcohol)–graphene oxide–polypyrrole composite hydrogel for elastic supercapacitors, *J. Mater. Sci.*, 2020, **55**, 11779–11791, DOI: 10.1007/s10853-020-04833-x.

53 H. Liu, Q. Zhao, K. Wang, Z. Lu, F. Feng and Y. Guo, Facile synthesis of polypyrrole nanofiber (PPyNF)/NiOx composites by a microwave method and application in supercapacitors, *RSC Adv.*, 2019, **9**, 6890, DOI: 10.1039/c8ra09666j.

54 L. J. van der Pauw, A method of measuring specific resistivity and Hall effect of discs of arbitrary shape, *Philips Res. Rep.*, 1958, **13**, 1–9.

55 A. Grumezescu and A. M. Holban, *Engineering Tools in the Beverage Industry: Vol 3: The Science of Beverages*, Woodhead Publishing, 2019.

56 S. Hestrin and M. Schramm, Synthesis of cellulose by Acetobacter xylinum. 2. Preparation of freeze-dried cells capable of polymerizing glucose to cellulose, *Biochem. J.*, 1954, **58**, 345, DOI: 10.1042/bj0580345.

57 A. F. Jozala, R. A. N. Pértile, C. A. dos Santos, V. d. C. Santos-Ebinuma, M. M. Seckler, F. M. Gama and A. Pessoa Jr., Bacterial cellulose production by Gluconacetobacter xylinus by employing alternative culture media, *Appl. Microbiol. Biotechnol.*, 2015, **99**, 1181–1190, DOI: 10.1007/s00253-014-6232-3.

58 P. Gatenholm and D. Klemm, Bacterial nanocellulose as a renewable material for biomedical applications, *MRS Bull.*, 2010, **35**, 208–213, DOI: 10.1557/mrs2010.653.

59 S.-P. Lin, I. L. Calvar, J. M. Catchmark, J. R. Liu, A. Demirci and K. C. Cheng, Biosynthesis, production and applications of bacterial cellulose, *Cellulose*, 2013, **20**, 2191–2219, DOI: 10.1007/s10570-013-9994-3.

60 T. T. Nge, J. Sugiyama and V. Bulone, Bacterial cellulose-based biomimetic composites, in *Biopolymers*, InTech, 2010, ch. 18.

61 J. George, K. V. Ramana, A. S. Bawa and Siddaramaiah, Bacterial nanocrystalline cellulose exhibiting high thermal stability and their polymer nanocomposites, *Int. J. Biol. Macromol.*, 2011, **48**, 50–57, DOI: 10.1016/j.ijbiomac.2010.09.013.

62 V. P. Puri, Effect of crystallinity and degree of polymerization of cellulose on enzymatic saccharification, *Biotechnol. Bioeng.*, 1984, **26**, 1219–1222, DOI: 10.1002/bit.260261010.

63 S. A. Ogundare, V. Moodley and W. E. van Zyl, Nanocrystalline cellulose isolated from discarded cigarette filters, *Carbohydr. Polym.*, 2017, **175**, 273–281, DOI: 10.1016/j.carbpol.2017.08.008.

64 S. A. Ogundare and W. E. van Zyl, Amplification of SERS "hot spots" by silica clustering in a silver nanoparticle/nanocrystalline-cellulose sensor applied in malachite green detection, *Colloids Surf., A*, 2019, **570**, 156–164, DOI: 10.1016/j.colsurfa.2019.03.019.

65 S. Mueller, C. Weder and E. J. Foster, Isolation of cellulose nanocrystals from pseudostems of banana plants, *RSC Adv.*, 2014, **4**, 907–915, DOI: 10.1039/C3RA46390G.

66 Y. R. Kang, Y. L. Li, F. Hou, Y. Y. Wen and D. Su, Fabrication of electric papers of graphene nanosheet shelled cellulose fibres by dispersion and infiltration as flexible electrodes for energy storage, *Nanoscale*, 2012, **4**, 3248–3253, DOI: 10.1039/C2NR30318C.

67 M. B. Heaney, Electrical Conductivity and Resistivity, in *Electrical Measurement, Signal Processing and Displays*, ed. J. G. Webster, CRC Press, 2003, ch. 7.